

# The expression of *UNC5D* is abnormal in the early stage of colorectal tumors associated with its proliferation and migration

L.-P. SHI<sup>1</sup>, C. ZOU<sup>1</sup>, L.-J. MAO<sup>2</sup>, T.-T. CHEN<sup>3</sup>, T. XIE<sup>4</sup>

<sup>1</sup>Good Clinical Practice Center, The Affiliated Hospital of Nanjing University of Chinese Medicine, Qinhuai District, Nanjing, Jiangsu, China

<sup>2</sup>Digestive Endoscopy Center, The Affiliated Hospital of Nanjing University of Chinese Medicine, Qinhuai District, Nanjing, Jiangsu, China

<sup>3</sup>The First Clinical Medical College, Nanjing University of Chinese Medicine, Nanjing, Jiangsu, China

<sup>4</sup>College of Medicine, Hangzhou Normal University, Yuhang District, Hangzhou, Zhejiang, China

*L.-P. Shi and C. Zou contributed equally to this study*

**Abstract. – OBJECTIVE:** Colorectal adenomas are an important precancerous lesion of colorectal adenoma with a high incidence. This study aims to explore new prognostic targets for colorectal adenomas through bioinformatics techniques.

**MATERIALS AND METHODS:** In this study, data from 29 colonic adenomas and 38 normal colonic mucosa in GSE37364 were analyzed to screen for differentially expressed genes (DEGs). Then, batch survival analysis, construction of risk model, mutation analysis, Cox regression analysis and expression analysis were performed on DEGs to determine the hub genes of this study. Finally, immune correlation analysis and cell experiments were carried out on the hub gene to explore its potential mechanism.

**RESULTS:** In our study, a total of 431 up-regulated and 809 down-regulated differentially expressed genes (DEGs) were identified. Among these, Unc-5 Netrin Receptor D (*UNC5D*) emerged as a pivotal gene associated with colorectal adenoma. Notably, *UNC5D* expression levels were found to be significantly higher in normal tissues compared to colorectal adenoma tissues. Furthermore, our analysis demonstrated that *UNC5D* showed promising diagnostic potential for patients with colon adenocarcinoma. *In vitro* experiments revealed that the overexpression of *UNC5D* had a profound impact on the behavior of colorectal tumor cells. Specifically, it led to a substantial reduction in the proliferation, motility, and invasion of these tumor cells. Additionally, *UNC5D* was shown to exert control over *STAT1/STAT3* phosphorylation, which in turn regulated the expression of *PD-L1* in response to interferon (*IFN*) stimulation. These findings highlight the significant

role of *UNC5D* in modulating immune responses and the development of colorectal adenoma. *UNC5D* emerges as a potential diagnostic biomarker and an attractive immunotherapeutic target in the context of colorectal malignancies. These results call for further exploration of *UNC5D*-based strategies for the diagnosis and treatment of colorectal adenoma and adenocarcinoma.

**CONCLUSIONS:** In addition to having the potential to be used as a diagnostic biomarker and an immunotherapeutic target in colorectal malignancies, *UNC5D* is necessary for the growth of colorectal adenomas. Additionally, *UNC5D* controlled *STAT1/STAT3* phosphorylation to suppress the growth of colorectal cancers by regulating *IFN*-induced *PD-L1* expression.

*Key Words:*

Colorectal adenomas, *UNC5D*, *IFN-γ*, *PD-L1*, *STAT1/STAT3* phosphorylation, Prognostic role, Survival relevance.

## Introduction

Colorectal adenomas are recognized as the precursors of colorectal cancers<sup>1</sup>. Its incidence and recurrence are related to the population aging, smoking, obesity<sup>2</sup>, excessive alcohol consumption, a low-fiber diet<sup>3,4</sup>, and so on. Endoscopic mucosal resection (EMR) for the removal of colorectal tumors is widely performed worldwide<sup>5</sup>. Although much progress has been made in modern medical technology, the problem of its high recurrence has not been solved yet. Vitamin D,

aspirin, cyclooxygenase-2 (COX-2) inhibitors, metformin, and calcium, are reported to have a certain effect on adenoma recurrence<sup>6,7</sup>. However, the therapeutic effect of the above methods is still controversial, with significant side effects under long-term use.

Early-stage cancers may allow less aggressive approaches, such as local excision (LE), to maintain quality of life without compromising tumor outcome. This study demonstrated excellent survival outcomes in patients with early rectal adenocarcinoma treated with LE alone<sup>8</sup>. However, colorectal adenomas can eventually develop into colon adenocarcinoma with the progression of carcinogenesis, which is caused by mutation accumulation and epigenetic alterations<sup>9,10</sup>. This process may require about 10-15 years, although in some cases, it may occur sooner, particularly in patients with Lynch syndrome<sup>11</sup>. Advances in high-throughput sequencing have provided new directions for cancer treatment<sup>12</sup>, which indicates that exploring genes with prognostic value of colorectal adenomas will help develop new therapeutic targets and improve patient risk stratification after clinical treatment<sup>13</sup>. For example, high-mobility group nucleosome-binding domain 5 (*HMGN5*) can increase the proliferative and migrative capacity of colorectal carcinoma cells *via* targeted binding to *FGF12*. In addition, clinical data analyses demonstrate that *HMGN5* is intimately related to the incidence rate of lymph node metastasis and distant metastasis in patients with colorectal carcinoma<sup>14</sup>. *CircRIP2* is a potential indicator for predicting tumor staging and distant metastasis of colorectal carcinoma. It aggravates the deterioration of colorectal carcinoma by negatively regulating *CBFB*<sup>15</sup>. In addition to high-throughput sequencing technology, a deeper understanding of biomolecular markers can also be used to predict disease progression and prognosis in colorectal cancer more accurately. For example, studies<sup>16</sup> have found that MutS homolog (*MSH*)-6 markers can be seen in CRC as mismatch repair gene deletions in young women with right-sided tumors, poorly differentiated and mucinous components using immunohistochemistry for both prophylactic and diagnostic purposes. There is also a link between clinical and pathological features of patients with *KRAS* marker status<sup>17</sup>. Furthermore, the development of colorectal adenomas is significantly influenced by the tumor micro-environment (TME), which is the site of tumor

cells' interactions with the human immune system. Researching this area may help create immunotherapies for this condition<sup>18,19</sup>.

In this study, we analyzed GSE37364 dataset in Gene Expression Omnibus (GEO) to screen DEGs related to colorectal adenomas. As colorectal adenomas could develop into colon adenocarcinoma, we analyzed the biological function of GSE37364-DEGs in The Cancer Genome Atlas (TCGA)-colon adenocarcinoma samples, and identified a new diagnostic biomarker, *UNC5D*, through bioinformatics analysis and cell experiments. These results may have implications for the comprehensive clinical application of patients with colorectal tumors.

## Materials and Methods

### Data Origination

Over 20,000 primary cancer and matched normal samples from 33 different cancer types were molecularly described by TCGA, a significant cancer genomics program. We downloaded 455 colon adenocarcinoma samples from the TCGA database for this study. Besides, GSE37364 (29 samples with colorectal adenoma and 38 samples of normal colonic mucosa were collected for this study) was included in the GEO database (<https://www.ncbi.nlm.nih.gov/geo/>) in the format of MINIML. The limma package of R software (version: 3.40.2, Vienna, Austria) was used to evaluate differential mRNA expressions. “ $p < 0.05$ , FC (fold change)  $> 2$  or  $FC < 0.5$ ” were defined as a threshold for up-regulation and down-regulation, respectively. To confirm the possible functions of candidate targets in further detail, DEGs were investigated by principal component analysis (PCA) and feature enrichment analysis. Gene Ontology (GO)<sup>20</sup> is a commonly used tool for annotating genes with functions, in the aspects of Molecular Functions (MF), Cellular Components (CC) and Biological Pathways (BP). Kyoto Encyclopedia of Genes and Genomes (KEGG)<sup>21</sup> was used to analyze gene function and related high-level genomic functional information.

### Search Tool for the Retrieval of the Interacting Gene/Protein Database (STRING)

STRING could design PPI networks of up- (Supplementary Figure 1) and down-regulated (Supplementary Figure 2) DEGs in colorectal

adenomas<sup>22</sup>. STRING can find proteins that interact directly with the input proteins, and then create PPI networks including these proteins and their interactions.

### ***Survival Analysis of the Genes in PPI***

Through batch survival analysis, the impact of genes on patient prognosis was examined<sup>23</sup>. The median gene expression is used as a grouping strategy to examine how the prognosis of several groups differs depending on the expression of a specific gene. Clinical data pertaining to 454 colon adenocarcinomas was retrieved from the TCGA dataset. After the log-rank test and univariate Cox regression, *p*-values and hazard ratios (HR) with 95% confidence intervals (CI) were produced for the Kaplan-Meier analysis. Statistics were considered significant for *p*-values under 0.05.

### ***Construction of the Risk Score Prognostic Model***

To identify genes associated with prognosis and create metabolic-related gene signatures, we used Lasso-Cox regression analysis<sup>24</sup>. Based on the median risk value, patients with colorectal adenoma were divided into low-risk and high-risk groups. The Kaplan-Meier survival curve and the log-rank test were used to evaluate the prognostic value. Additionally, we used the R package “survival ROC” to evaluate the prognostic importance of gene signatures over time.

### ***Gene Mutation Analysis***

To investigate the potential prognostic significance of copy number alterations (CNA) and single nucleotide variants (SNV) in colorectal adenocarcinoma (COAD), we analyzed the CNA and SNV percentages of 28 prognostic genes. The CNA percentage was calculated as the ratio of the number of patients with a CNA in a particular gene to the total number of patients in the cohort, multiplied by 100. We created a heatmap based on the SNV percentage to study the 28 prognostic genes in COAD's SNV distribution further. The heatmap was generated using the R software package “maftools”, which provides comprehensive visualization and analysis of somatic mutations. To obtain a comprehensive view of somatic mutations in COAD patients, we utilized the “maftools” package to download and visualize somatic mutations in the cohort. The resulting data were presented in multiple formats, including oncoplots, waterfall plots, and mutation burden plots.

### ***Expression and ROC Curve Analysis of Top 10 Mutated Genes in Adenomas and Normal Tissues***

We used box plots to examine the expression levels of the top 10 mutant genes in adenomas and normal tissues in order to look into the possible diagnostic utility of these genes. The expression data were obtained from a publicly available gene expression dataset, and the box plots were generated using R software. In order to evaluate the diagnostic efficacy of the top 10 mutant genes, receiver operating characteristic (ROC) curves were built. Genes with AUC values above 0.9 were deemed to have high diagnostic accuracy. The area under the ROC curve (AUC) was calculated. To further explore the diagnostic potential of the highly accurate genes, we generated a forest plot to visualize their diagnostic performance.

### ***The Immunoassay on UNC5D***

We compared the immune cell expression between *UNC5D* high expression and low expression groups using the “immunedeconv” software package in order to examine the potential function of *UNC5D* in controlling immune cell infiltration in colon cancer. We created boxplots to evaluate the immune cell enrichment fraction between *UNC5D* high expression and low expression groups in order to further investigate the association between *UNC5D* expression and immune cell enrichment. We examined the levels of eight immune checkpoint-related genes in tumor and normal tissues in order to look into the potential clinical importance of *UNC5D* in CRC. The boxplots were produced using R software, and the expression data were taken from the TCGA database.

### ***Cell Culture and Transfection***

Human colon adenocarcinoma cells (DLD-1, SW480, HCT116, RKO) and normal colon cells (NCM460) were obtained from the American Type Culture Collection (ATCC) and maintained in Dulbecco's Modified Eagle Medium (DMEM) supplemented with 10% fetal bovine serum (FBS) and 1% penicillin-streptomycin (PS) at 37°C in a humidified incubator with 5% CO<sub>2</sub>. Cells were seeded in 6-well plates and transfected with *UNC5D* overexpression plasmid or empty vector using Lipofectamine 2000 according to the manufacturer's instructions.

**Quantitative Real-Time PCR (qRT-PCR)**

We prepared the reverse transcription system (10 µl RT system per sample) on ice (Novozymes reagent), 2 µl RT reagent + 7 µl diethyl pyrocarbonate (DEPC) water + 1 µl RNA, and put it into the reverse transcription instrument for 15 min. The reverse transcription conditions were 37°C, 15 min, 85°C to obtain a cDNA solution, which was stored at -20°C. The remaining samples were stored at -80°C. The preparation of the PCR system was carried out on ice. Upstream primer (10 nmol/ul), downstream primer (10 nmol/ul), SYBER green (2×), and DEPC water were prepared according to 1:1:7.5:4.5 and shaken well. We added 14 µl of the PCR reaction solution to each well of the PCR plate. We removed the cDNA, shook it quickly, and added 1 µl of sample per well to the PCR plate. The PCR plate was sealed with sealing film and centrifuged for 1 min. We put the PCR plate into the PCR machine (EZBioscience, Roseville, MN, USA) and used the standard three-step method to carry out the PCR reaction: Stage 1: Pre-denaturation: 95°C, 10 sec; Stage 2: PCR reaction: 95°C, 10 sec; Tm/60°C, 30 seconds; 72°C, 30 seconds, 40 cycles; Third stage: melting curve analysis: 95°C, 15 sec; 70°C, 15 seconds. The semi-quantitative analysis of RT-PCR used the Livak method. The amplification efficiencies of inflammatory target genes and internal reference genes were close to 100% during the experiment, and the deviations of each other's efficiencies were within 5%.

**Western Blotting (WB)**

By utilizing RIPA lysis buffer (Thermo Fisher, Waltham, MA, USA) enhanced with protease and phosphatase inhibitors, the protein was recovered from cells. The BCA protein assay kit was used to calculate the protein concentration. SDS-PAGE was used to separate equal amounts of protein, which was then deposited onto PVDF membranes (Millipore; Darmstadt, Germany). The membranes were treated with primary antibodies against *UNC5D*, *PD-L1*, *STAT1*, *STAT3*, and *GAPDH* overnight at 4°C after being blocked with 5% non-fat milk. After being washed, the membranes were treated for an hour at room temperature with secondary antibodies conjugated with horseradish peroxidase (HRP). Protein was detected by using the Electrochemiluminescence system (Millipore) on autoradiography film (Kodak; Rochester, NY, USA) or ChemiDoc Touch (Bio-rad; Hercules, CA, USA) and ImageJ (<https://imagej.net/ij/download.html>) was used to analyze them.

**Cell Proliferation Assay**

The Cell Counting Kit-8 (CCK-8) was used to measure cell proliferation in accordance with the manufacturer's recommendations. In 96-well plates, cells were seeded and cultivated for 0, 24, 48, 72, and 96 hours. Each well was then filled with CCK-8 solution, which was then incubated for two hours at 37°C. With the use of a microplate reader (Biotek, Synergy H1, Vermont, USA), the absorbance at 450 nm was calculated.

**Cell Migration and Invasion Assay**

Cell invasion and migration were assessed using Transwell chambers. Briefly, cells were sown in DMEM without serum in the upper chamber and DMEM with 10% FBS in the lower chamber. The upper chamber was pre-coated with Matrigel for the invasion assay. The cells on the membrane's upper side were removed after the first 24 hours of incubation, and the cells on its lower surface were then fixed with 4% paraformaldehyde and stained with crystal violet (Sinopharm Chemical Reagent, China), the migratory or invading cells were counted.

**Statistical Analysis**

The measurement data were represented as mean and standard deviation, and the experimental data were statistically evaluated and plotted using GraphPad Prism 9.0 software (<https://www.graphpad.com/updates/prism-900-release-notes>). The means of several groups that matched the criteria for normal distribution and homogeneity of variance were compared using a one-way analysis of variance, and further pairwise comparisons were made using the least significant difference method (LSD). For data with uneven variance, Dunnett's t3 test was applied. Statistical significance was determined by  $p < 0.05$  and  $p < 0.01$ , respectively.

**Results****Identification of DEGs from GSE37364**

The normalized expression values of mRNA in 67 samples in GSE37364 are shown in Figure 1A. Then, PCA plots showed the separation between colorectal adenoma samples and normal samples in GSE37364 (Figure 1B). The heat map of colorectal adenoma is shown in Figure 1C;

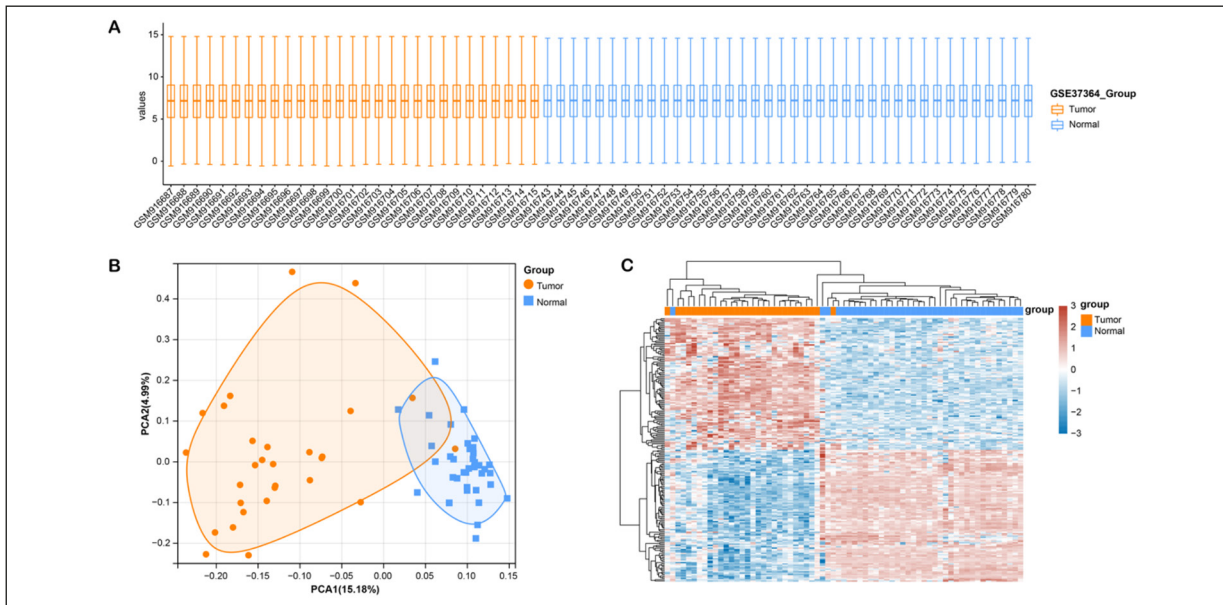


**Figure 1.** Identification of DEGs from GSE37364. **A**, Boxplot after data normalization, different colors represent different datasets, rows represent samples, and columns represent gene expression values in samples. **B**, PCA results before GSE37364 removal (PCA1: 15.18%, PCA2: 4.99%). **C**, Heat map of differential gene expression, red columns represent colorectal adenomas samples, and green columns represent normal control samples.

we obtained 431 up-regulated DEGs ( $p < 0.05$ ,  $FC > 2$ ) and 809 down-regulated DEGs ( $p < 0.05$ ,  $FC < 0.5$ ).

### GO, KEGG and PPI Network Analyses on DEGs

In KEGG pathways, the up-regulated DEGs were mostly related to the IL-17 signaling pathway, cytokine-cytokine receptor interaction, etc. (Figure 2A), and the down-regulated DEGs were mainly enriched in mineral absorption, protein digestion, and absorption etc. (Figure 2C). In GO terms, the up-regulated DEGs were chiefly enriched in response to drugs, cellular response to chemokine, etc. (Figure 2B). The down-regulated DEGs were mainly related to cellular divalent inorganic cation homeostasis, second-messenger-mediated signaling, etc. (Figure 2D). The PPI network for up-regulated DEGs consisted of 340 nodes and 1,144 edges (Supplementary Figure 1), while the PPI network for down-regulated DEGs comprised 718 nodes and 2,645 edges (Supplementary Figure 2). Nodes represented genes, and edges represented associations between genes. These genes were all used for the subsequent batch survival analysis.

### Batch Survival Analysis

Next, we used all DEGs in the PPI network for batch overall survival (OS) analysis, and finally, 59 OS plots with significant  $p$ -values ( $p < 0.05$ ) were acquired (Supplementary Figures 3, 4, 5). These genes have had a considerable influence on the prognosis of colon cancer patients.

### Establishment of Risk Score Prognostic Model

Then, the 59 genes with significant  $p$ -values ( $p < 0.05$ ) were used to design the optimal gene signature (Figure 3A, 3B). To identify gene signatures suitable for predicting survival in colon adenocarcinoma, patients were split into low-risk ( $N=227$ ) and high-risk groups ( $N=227$ ), based on the median risk score. On the distribution of survival status and time for each patient, a split line indicating the risk score threshold was displayed, and the bottom panel featured a heat map of the 28 important genes with a significant  $p$ -value (Figure 3C). The Kaplan-Meier curve showed that high-risk patients were connected with worse OS (Figure 3D). In addition, ROC curves showed the AUC for the predictive colon adenocarcinoma model at 1, 3, and 5 years was 0.806, 0.792, and 0.878 in the training set, respectively (Figure 3E).

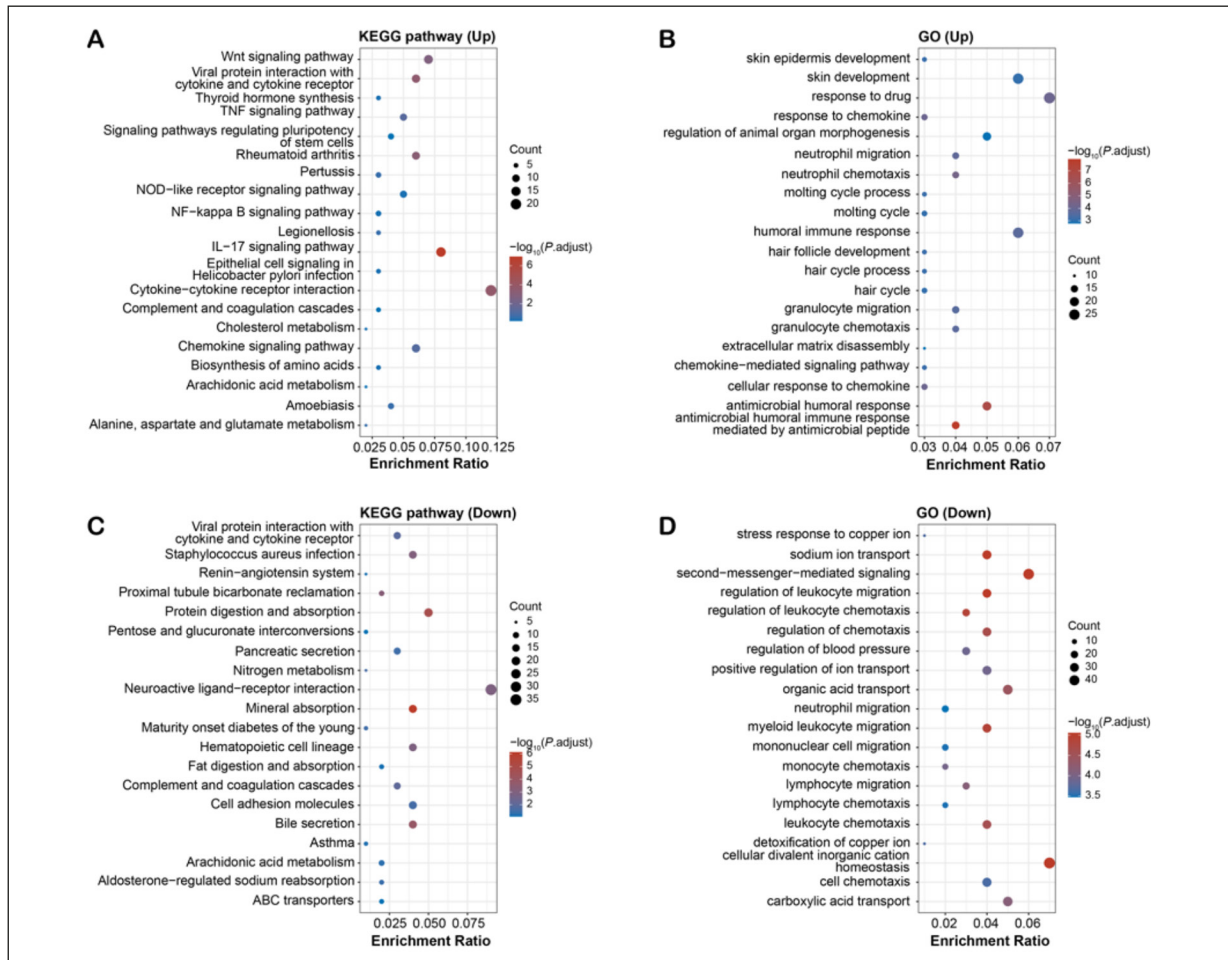


**Figure 2.** Functional enrichment analysis. **A**, and **C**, KEGG pathway results for up-regulated and down-regulated DEGs, respectively. The abscissa indicates the gene enrichment ratio, and the ordinate indicates the different pathways of gene enrichment. **B**, and **D**, GO term results of up-regulated and down-regulated DEGs, the larger the point, the greater the number of enriched genes.

### The Mutational Landscape Analysis of Signature Genes in Colon Adenocarcinoma

Mutational landscape analysis is an important tool for understanding the genetic alterations driving tumor progression and providing prognostic information in colon adenocarcinoma. Our results indicated that the dominant mutation types in these genes were heterozygous amplifications and heterozygous deletions, as shown by CNV analysis (Figure 4A). SNV heatmap analysis showed that mutation frequency increased with darker color intensity, suggesting a correlation between mutation frequency and tumorigenesis (Figure 4B). Panel summary plots illustrate the distribution of variants according to variant class, type, and SNV category, with mutational load for each sample shown at the bottom (left to right).

Stacked bar graphs show the top 10 mutated genes in colon adenocarcinoma (Figure 4C), while oncoplots depict the somatic landscape of CRC tumor samples, with missense mutations being the dominant mutation type (Figure 4D).

### The Expression and Diagnostic Value of Top 10 Mutated Genes

The expression levels of the top 10 mutated genes (*CAPN12*, *FZD3*, *LZTS3*, *MIER3*, *NLG1*, *PCDH9*, *SALL1*, *UNC5D*, *WDR72*, and *ZBTB7C*) showed significant differences between adenoma and normal tissues (Figure 5A), indicating their potential roles in the development of colorectal adenoma. ROC curve analysis revealed that seven genes (*CAPN12*, *FZD3*, *LZTS3*, *MIER3*, *PCDH9*, *UNC5D*, and *WDR72*) had AUC values above 0.9, indicating high diagnostic accuracy (Figures 5B-

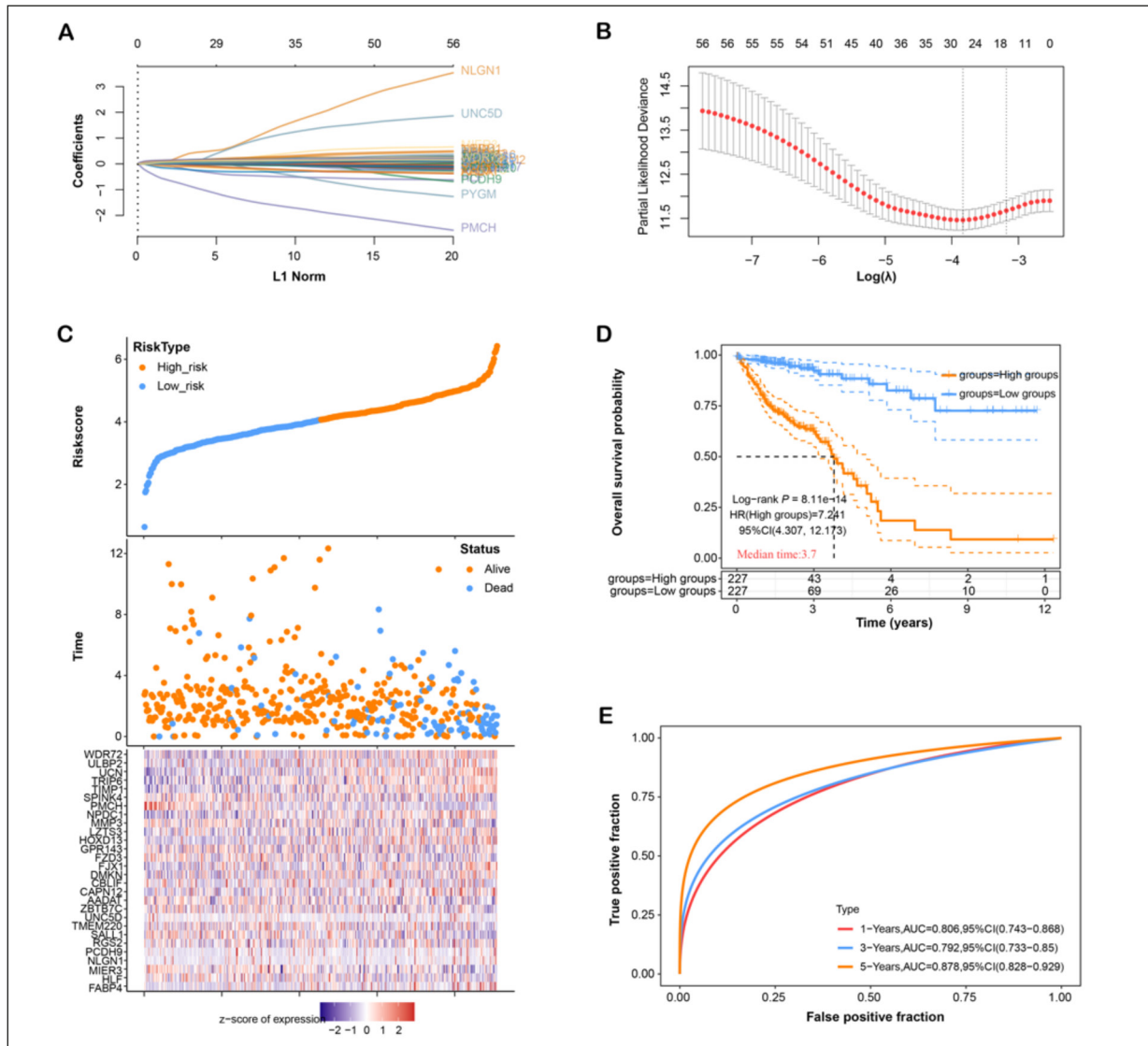


**Figure 3.** Establishment of prognostic model based on colorectal adenomas. **A**, LASSO-Cox regression algorithm, genes are represented by lines of different colors. **B**, Partial likelihood bias vs.  $\log(\lambda)$  in a LASSO-Cox regression model. **C**, Risk score distribution for patient OS and signature. Scatter plot of OS in patients with colorectal adenocarcinoma. Heat map of genes with significant  $p$ -values. **D**, Kaplan-Meier survival analysis shows differences between high- and low-risk groups. **E**, Time-dependent ROC curve analysis for 1-, 3-, and 5-year OS predictions using signatures based on significant  $p$ -value genes.

K). Further, forest plot analysis showed that these genes had high sensitivity and specificity (Figure 5L). Since *UNC5D* had not been reported in colorectal adenoma before, we chose *UNC5D* for further analysis.

### The Immunoassay on *UNC5D* in Colon Adenocarcinoma

From the results of immune analysis, among the 24 immune cells, natural killer (NK) cell resting, T cell CD8<sup>+</sup>, NK cell activated, B cell plasma, T cell CD4<sup>+</sup> memory resting, Macrophage

M2, and monocyte were significantly distributed in samples with different expressions of *UNC5D* (Figure 6A). Figure 6B displays the findings of the CIBERSORT algorithm's evaluation of the infiltration abundance of 22 tumor-infiltrating immune cells in the samples. Additionally, the enrichment scores of Mast cells, Eosinophils, B cells, T helper cells, Tcm, and TFH were significantly higher in *UNC5D* high expression (Figure 6C). Finally, the immune checkpoint gene *CD274* showed differences in the two samples by boxplot analysis (Figure 7D;  $*p < 0.05$ ).

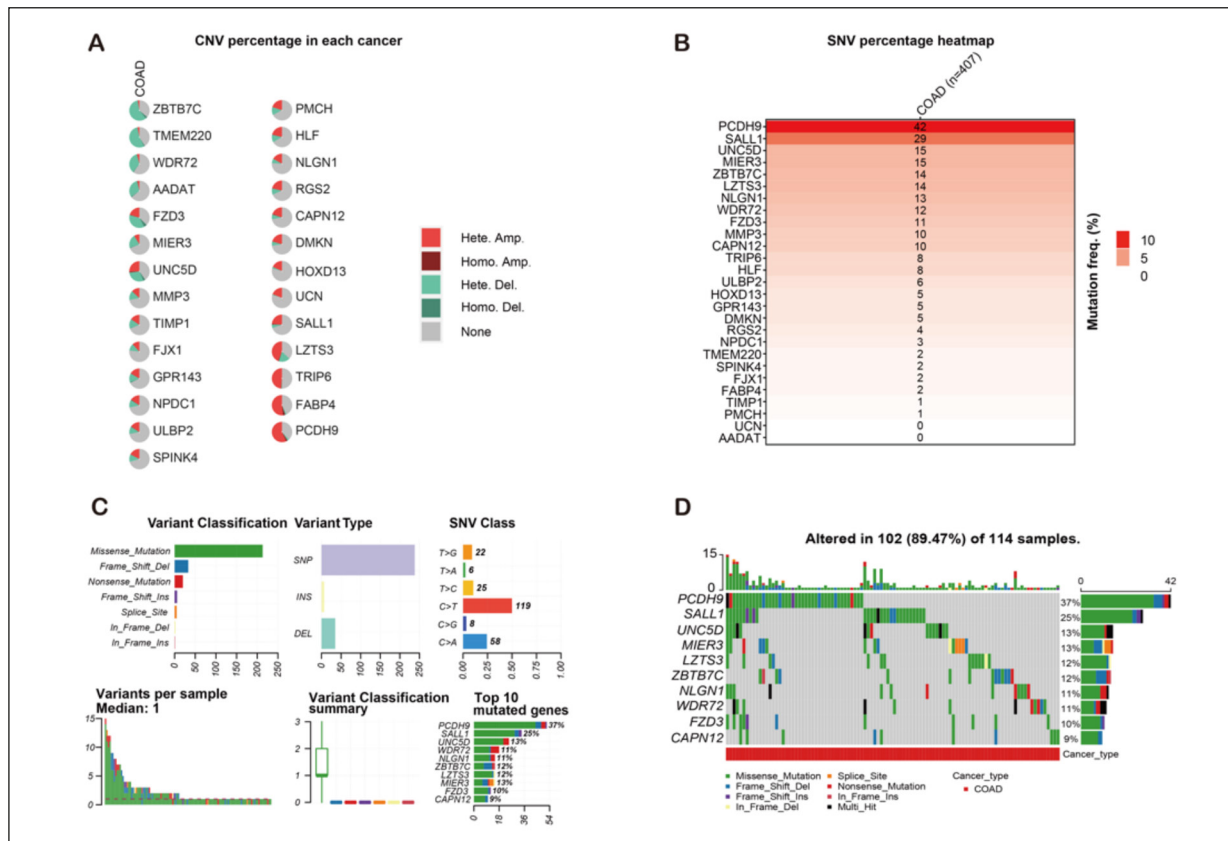


**Figure 4.** Mutational landscape analysis. **A**, CNV analysis of colorectal adenoma prognostic genes revealed that the main mutation types were heterozygous amplification and heterozygous deletion. **B**, SNV heatmap showed a positive correlation between SNV frequency and tumorigenesis, with darker colors indicating higher frequencies. **C**, Panel summary plot illustrated variant distribution according to variant class, type, and SNV class, with mutational load for each sample shown at the bottom (left to right). Stacked bar graph showing the top 10 mutated genes and their respective mutation frequencies in colorectal adenomas. **D**, The oncoplots depicted the somatic landscape of CRC tumor samples, with missense mutations being the dominant mutation type. Each line represents a tumor sample, and the height of the line represents the total number of somatic mutations present in that sample.

### ***UNC5D Inhibits HCT116 and RKO Cell Proliferation, Migration and Invasion In Vitro***

In *in vitro* experiments, we detected low expression levels of *UNC5D* in colorectal adenoma cells using qRT-PCR and WB experiments (Figure 7A and 7B). After *UNC5D* overexpression, both mRNA and protein levels were noticeably increased (Figures 7C and 7D). In addition, the overexpression of *UNC5D* detected by the CCK-8 assay significantly inhibited the proliferation of colorectal adenoma cells (Figure 7E and 7F). Likewise, overexpression of *UNC5D* resulted in reduced numbers of migratory and invasive colonic adenoma cells compared to controls in Transwell assays (Figure 7G and 7H). These findings imply that *UNC5D* may function as a

tumor suppressor gene in colorectal cancers, preventing cell proliferation, migration, and invasion.

### ***Overexpression of UNC5D Attenuates IFN- $\gamma$ -Induced PD-L1 Expression***

*TFN-* is an immune cell cytokine that is essential for the immune system's response to infections and malignancies<sup>25</sup>. *PD-L1* is a protein found on the surface of certain cells that plays a role in regulating immune responses<sup>26,27</sup>. In this study, we detected increased expression of *PD-L1* in colon adenocarcinoma cells treated with *TFN-* $\gamma$  using WB (Figure 8A). Subsequently, we investigated the effect of *UNC5D* overexpression and *IFN-* $\gamma$  treatment on the expression of *PD-L1* and *UNC5D* in colorectal adenoma cells. Based on the

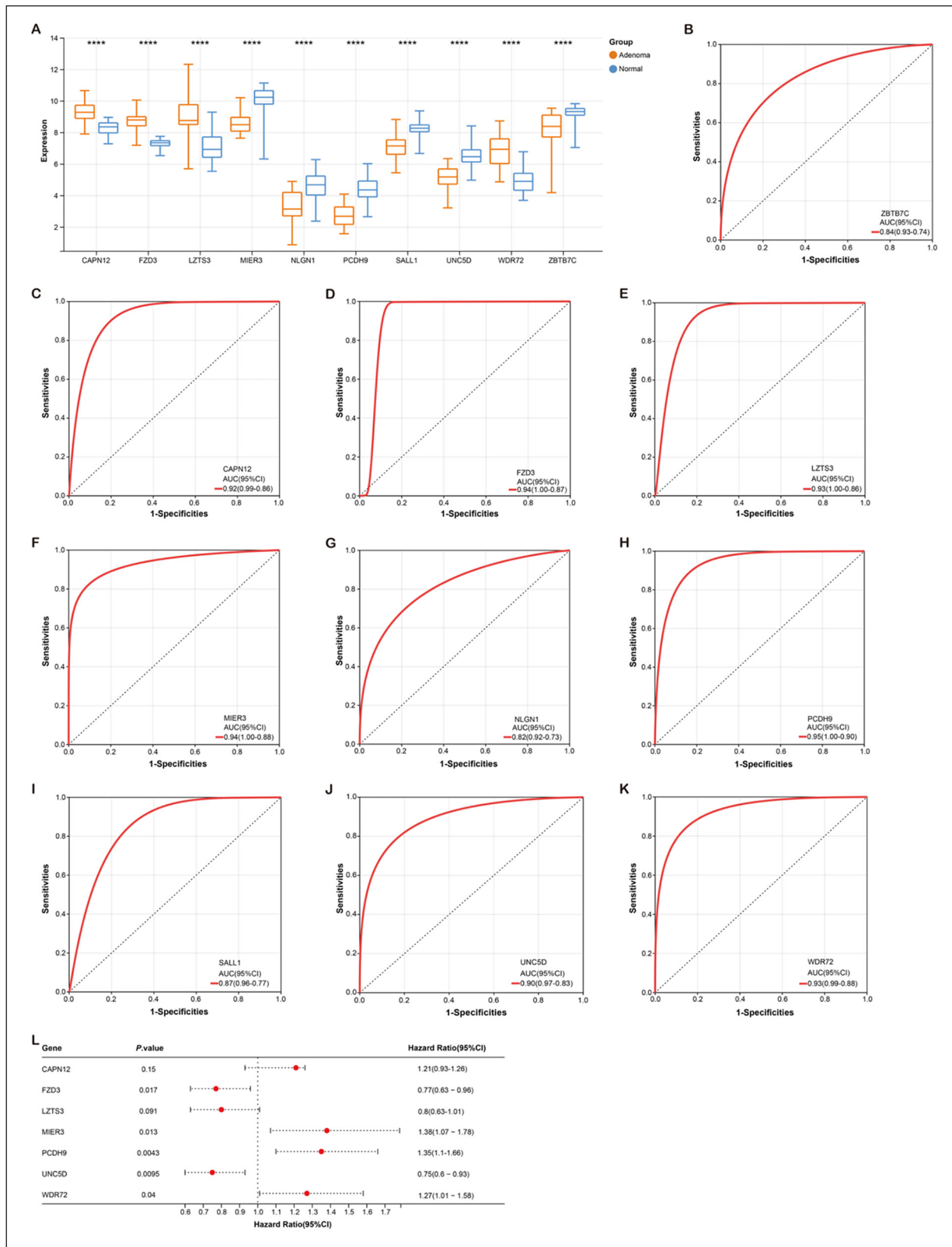


**Figure 5.** Differential expression of Top 10 mutated genes in colorectal adenomas. **A**, Boxplots of the expression levels of the top 10 mutated genes (*CAPN12*, *FZD3*, *LZTS3*, *MIER3*, *NLGN1*, *PCDH9*, *SALL1*, *UNC5D*, *WDR72*, and *ZBTB7C*) in adenoma and normal tissues. **B-K**, ROC curves of 10 mutated genes. **L**, Forest plot of 7 genes with AUC values above 0.9. \*\*\*\* $p < 0.0001$ .

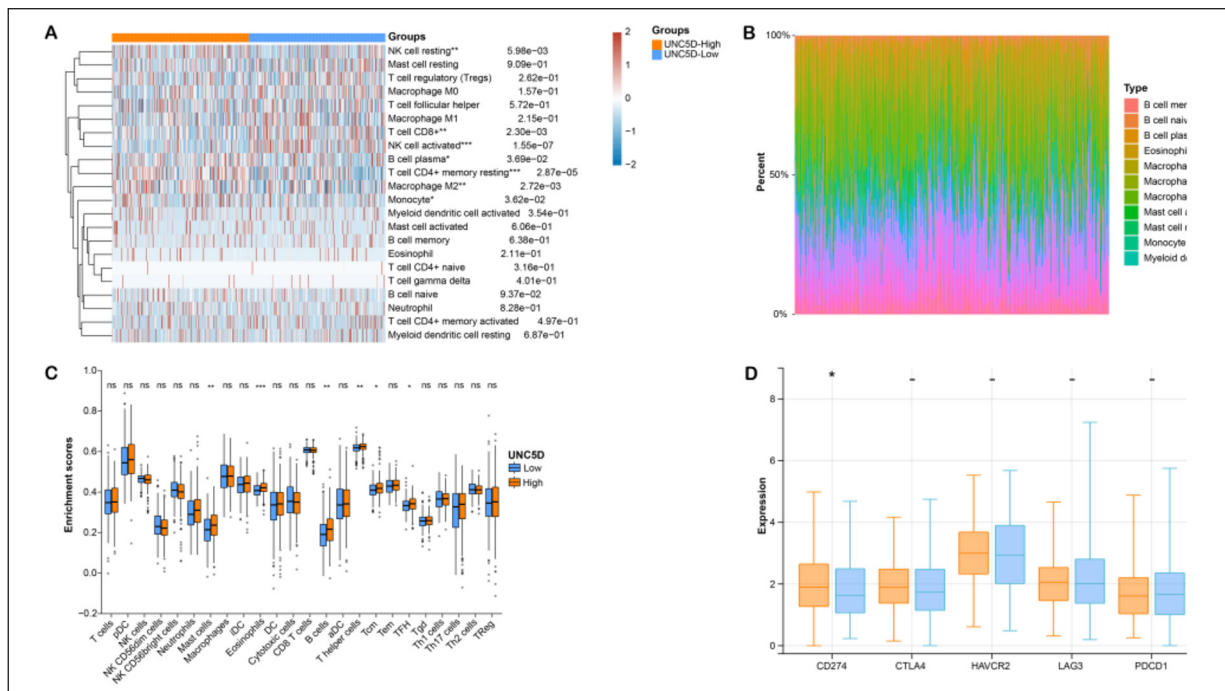


**Figure 6.** The immunoassay on *UNC5D* in colorectal adenoma. **A**, Heat map of 24 immune cell scores. \* $p < 0.05$ , \*\* $p < 0.01$  and \*\*\* $p < 0.001$ . **B**, The percentage abundance of 22 tumor-infiltrating immune cells in each sample. **C**, Enrichment fractions of high and low expression of *UNC5D* in 24 immune cells, respectively. **D**, Boxplot of expression levels of immune checkpoint genes in tumor and normal groups.

results of WB and qRT-PCR, we found that the expression of *UNC5D* was decreased after *TFN-γ* treatment. Furthermore, overexpression of *UNC5D* resulted in increased expression of *UNC5D*, which was rescued by concomitant treatment with *TFN-γ*. However, the expression of *PD-L1* was increased in cells treated with *TFN-γ*. Conversely, upregulation of *UNC5D* expression decreased *PD-L1* expression (Figure 8B-8G). This suggests that overexpression of *UNC5D* could attenuate *IFN-γ*-induced *PD-L1* expression in colorectal tumor cells.

### ***UNC5D* Regulates *IFN-γ*-Induced *PD-L1* Expression by Activating the Phosphorylation of *STAT1/STAT3***

*STAT1* and *STAT3* are transcription factors that are crucial for controlling cancer and immunological responses<sup>28</sup>. In this study, we looked at how *UNC5D* affects the expression of *PD-L1* in colorectal tumor cells, as well as how *STAT1* and *STAT3* are regulated. In colorectal carcinoma cells treated with *IFN-γ*, WB analysis revealed that *UNC5D* overexpression dramatically increased *STAT1* and *STAT3* protein expression levels (Figure 9A). Subsequently, we knocked

down *STAT1* and *STAT3* expression in these cells and found that the protein expression levels of *STAT1*, *STAT3*, and *PD-L1* were reduced after *IFN-γ* treatment (Figure 9B and 9C). This suggests that *STAT1* and *STAT3* may be involved in the regulation of *UNC5D* on *PD-L1* expression in colorectal tumor cells.

## **Discussion**

Currently, we analyze 67 samples in the GSE37364 dataset to identify DEGs associated with colorectal adenomas. Afterward, a series of bioinformatics analyses and qRT-PCR detection were performed on these DEGs, and finally, a key gene associated with colorectal adenoma, *UNC5D*, was screened. Next, the expression levels of *UNC5D* in colorectal tumors were studied, and the correlation between *UNC5D* and immune cells was also evaluated. Besides, we explored the potential mechanism of *UNC5D* in colorectal tumors.

From the GSE37364 dataset, we examined 431 up-regulated genes and 809 down-regulated DEGs. We were then able to comprehend the

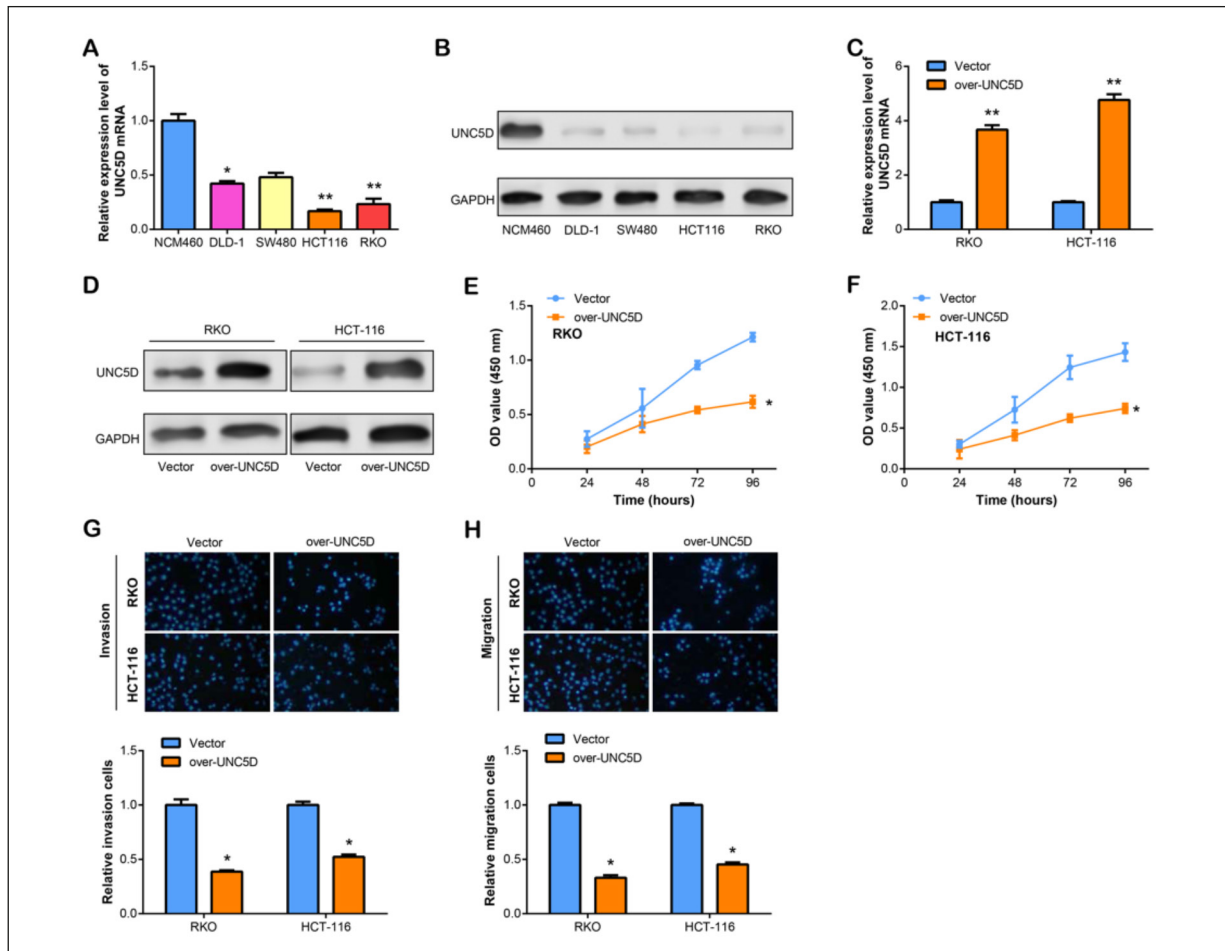


**Figure 7.** Analysis of the regulation of *UNC5D* on the proliferation, migration and invasion of colorectal adenoma cells. **A-B**, qRT-PCR and WB analysis of *UNC5D* mRNA/protein expression levels in normal colorectal cells and colorectal adenoma cells. **C-D**, qRT-PCR and WB were used to detect the overexpression efficiency of *UNC5D* in colorectal adenoma cells, respectively. **E-F**, CCK-8 assay showing the effect of *UNC5D* overexpression on the proliferation of colorectal adenoma cells. **G-H**, Representative images of a Transwell assay showing the effect of *UNC5D* overexpression on invasion and migration of colorectal adenoma cells. \* $p < 0.05$ , \*\* $p < 0.01$ , \*\*\* $p < 0.001$ .

important keywords and pathways associated with colorectal adenomas and improved our understanding of the pathophysiology and preventative strategies of colorectal adenomas by doing KEGG and GO enrichment analysis on the DEGs. In the GO category, the up-regulated DEGs were enriched in response to drugs. Harvie<sup>29</sup>'s research shows that the use of drugs like nutritional supplements can cause some significant adverse effects in cancer patients. For example, vitamin E will deteriorate prostate cancer and colorectal adenomas. Harvie<sup>29</sup> believes that nutritional supplements suitable for one's genetics, diet, tumor histology, and treatment are beneficial for the recovery of patients. Additionally, other enriched treatments include cellular response to chemok-

ine. Doll et al<sup>30</sup> tested the modulation of chemokine expression on various stimuli in 97 patients with complete colorectal adenoma resection. The results suggest that the chemokine family is specifically upregulated in colorectal cancer. Moreover, down-regulated DEGs were associated with the regulation of leukocyte migration, blood pressure, leukocyte chemotaxis, cell chemotaxis, and so on. Liu et al<sup>31</sup> identified the enrichment functions and pathways of the DEGs that were associated with colorectal cancer. Liu et al<sup>31</sup> suggest that DEGs were mainly related to leukocyte chemotaxis, chemokine receptor binding, and positive regulation of cytokine secretion. Yin et al<sup>32</sup> found that DEGs related to colorectal cancer were mainly enriched in leukocyte chemotaxis, cell chemo-

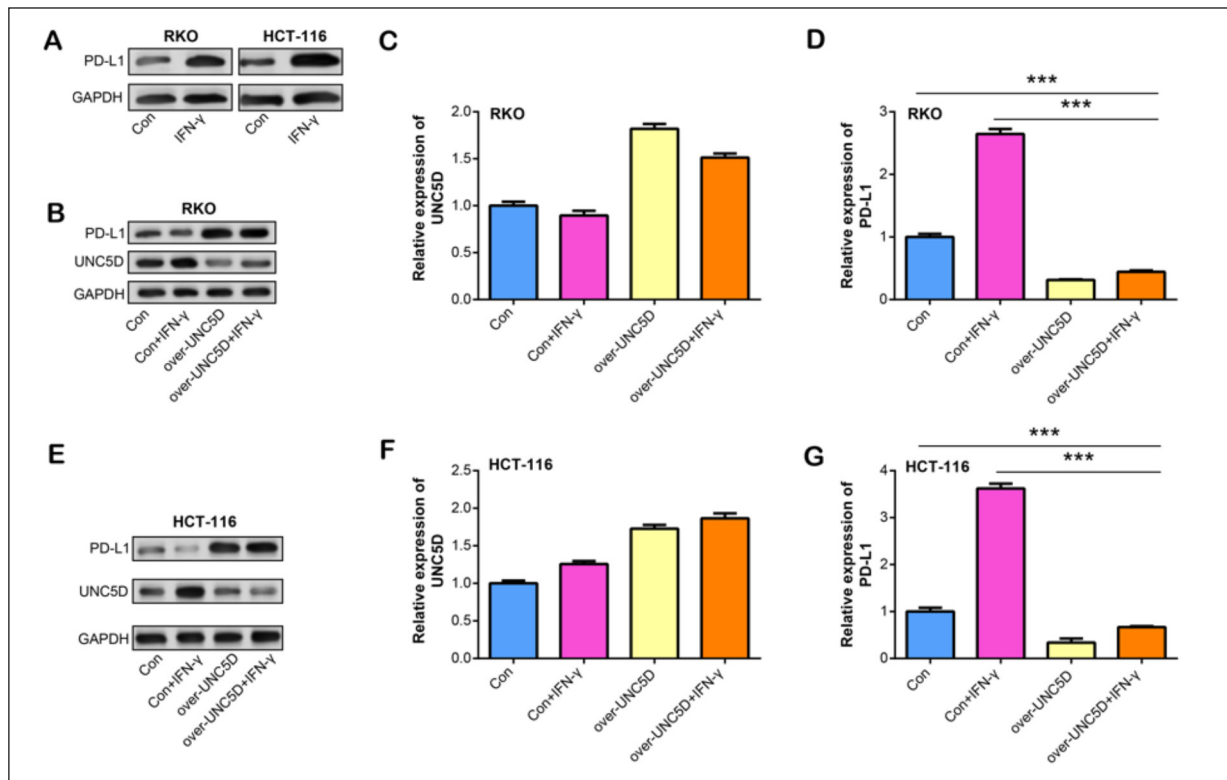


**Figure 8.** WB and qRT-PCR analysis of the effect of *UNC5D* overexpression on IFN- $\gamma$ -induced PD-L1 expression in colorectal adenoma cells. **A**, WB analysis of PD-L1 expression in colorectal adenoma cells treated with IFN- $\gamma$ . **B**, **E**, WB detection of protein expression levels of PD-L1 and *UNC5D* after overexpression of *UNC5D* before and after IFN- $\gamma$  treatment in colorectal adenoma cells. **C**, **F**, qRT-PCR analysis of *UNC5D* mRNA expression in colorectal adenoma cells before and after IFN- $\gamma$  treatment with or without *UNC5D* overexpression. **D**, **G**, qRT-PCR analysis of PD-L1 mRNA expression in colorectal adenoma cells before and after IFN- $\gamma$  treatment with or without *UNC5D* overexpression. Observation of cells using a microscope at 20X magnification. \*\*\* $p < 0.001$ .

taxis, and retinoic acid metabolic process. Wu et al<sup>33</sup> found that the genes associated with colorectal cancer were chiefly enriched in the regulation of leukocyte migration and regulation of protein secretion. These findings indicate these *DEGs* are connected with various regulations of the human body system.

As for the KEGG analysis, the up-regulated *DEGs* were related to the *Wnt* signaling pathway, thyroid hormone synthesis, and *TNF* signaling pathway. Tian et al<sup>34</sup> have shown that the *Wnt*/ $\beta$ -catenin pathway regulates the self-renewal of intestinal stem cells, and its persistent signaling causes intestinal epithelial cell hyperprolif-

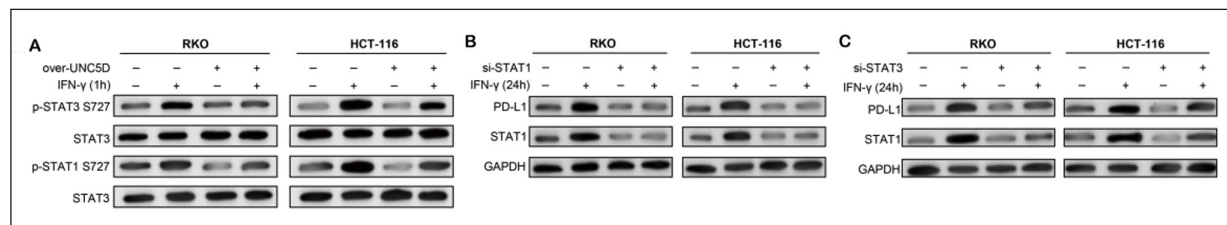


**Figure 9.** *UNC5D* regulates the expression of STAT1 and STAT3 and affects PD-L1 expression in colorectal adenoma cells. **A**, WB analysis of the protein expression levels of STAT1 and STAT3 in colorectal adenoma cells treated with IFN- $\gamma$  after *UNC5D* overexpression. **B**, WB analysis of the protein expression levels of STAT1, and PD-L1 in colorectal adenoma cells treated with IFN- $\gamma$  after knockdown of STAT1 expression. **C**, WB analysis of the protein expression levels of STAT3, and PD-L1 in colorectal adenoma cells treated with IFN- $\gamma$  after knockdown of STAT3 expression.

eration and neoplastic transformation, resulting in the development of colorectal cancer. Their findings<sup>34</sup> confirm that *HMGA2* and *Wnt/β-catenin* have critical and synergistic roles in the carcinogenesis of colorectal adenomas. Besides, the findings of Boursi et al<sup>35</sup> demonstrate that thyroid hormone replacement (*THR*) users have a lower risk of colorectal cancer, whereas patients with hyperthyroidism or hypothyroidism who are not receiving thyroid hormones have a higher risk. The protective association of *THR* increases with treatment duration and cumulative dose, higher in patients undergoing colectomy and more pronounced in women. The down-regulated DEGs were enriched in *staphylococcus aureus* infection and mineral absorption. By thoroughly evaluating DEGs and genomes and using several testing adjustments, the *Staphylococcus aureus* infection pathway and the *IgA* production pathway of the gut immune network were highlighted to be closely associated with colorectal adenomas<sup>36</sup>. Previous research<sup>37</sup> has shown that the mineral selenium can prevent the development of colorectal tumors. In the study by Helm et al<sup>37</sup>, lower plasma selenium levels were associated with multiple adenomas but irrelevant to adenoma size or location. They also suggested that selenium was protective against colorectal adenomas and might be a potentially useful chemo-preventive agent for colorectal tumors.

Following that, we filtered out a key gene, Gene-Unc-5 Netrin Receptor D (*UNC5D*), by performing a PPI network, survival curve, LASSO-Cox analysis, and others on DEGs. According to this study, *UNC5D* played as a tumor suppressor gene in colorectal tumors and was lowly expressed in adenoma tissue, and high *UNC5D* expression was associated with a higher survival rate. In Lu et al<sup>38</sup> and Dong et al<sup>39</sup> studies, *UNC5D* is a recently-discovered member of the *UNC5* family, and it is a suppressive gene in a variety of malignancies, like renal cell carcinoma and bladder cancer. According to their final findings, *UNC5D* may be a viable biomarker for diagnosing and treating metastatic prostate cancer. Besides, Zhang et al<sup>40</sup> demonstrate that *UNC5D*, as a suppressive gene, is related to the tumor aggressiveness of thyroid cancer. According to a previous study<sup>41</sup>, *UNC5D* can activate the activity of the netrin receptor and participate in intercellular adhesion through plasma membrane adhesion molecules. Uhan et al<sup>42</sup> found that *KCNA1* and *UNC5D* have the potential to be diagnostic biomarkers in patients with early-stage colorectal cancer.

*In vitro* results of this study demonstrate that *UNC5D* functions as a tumor suppressor gene in colorectal tumors, inhibiting cell proliferation, migration, and invasion. Additionally, the overexpression of *UNC5D* partially attenuates *IFN-γ*-induced *PD-L1* expression in colorectal tumor cells. By controlling the phosphorylation of *STAT1/STAT3*, *UNC5D* controls the phosphorylation of *IFN*-induced *PD-L1* expression. This work sheds new information on the immune response control in colorectal tumor cells and underlines the potential of *UNC5D* as a therapeutic target in colorectal adenoma. Given that *PD-L1* is upregulated in colorectal tumor cells treated with *IFN-γ*, it is possible that *PD-L1* contributes to the immune response to colorectal malignancies. The ability of *UNC5D* to partially attenuate *IFN-γ*-induced *PD-L1* expression suggests that *UNC5D* may be involved in the regulation of immune responses in colorectal tumor cells. The role of *STAT1* and *STAT3* in the regulation of immune responses and tumorigenesis has been well-established, and this study provides further evidence of their involvement in the regulation of *PD-L1* expression in colorectal tumors. The results suggest that the regulation of *STAT1* and *STAT3* by *UNC5D* may be a potential mechanism underlying the tumor suppressive effects of *UNC5D* in colorectal tumors.

## Conclusions

Overall, we obtained a promising gene, *UNC5D*, necessary for the growth of colorectal adenomas. This gene may be a therapy target for colorectal adenomas since it is expressed at a reduced level in these tumors as compared to nearby normal tissues. By survival analysis, high *UNC5D* expression indicated a better prognosis in colorectal tumor patients, and *UNC5D* could be a diagnostic biomarker for colorectal tumor patients. Additionally, *UNC5D* controlled *STAT1/STAT3* phosphorylation to suppress the growth of colorectal cancers by regulating *IFN*-induced *PD-L1* expression. These results imply a significant function for *UNC5D* in the control of immune response and carcinogenesis in colorectal adenoma.

## Conflict of Interest

The authors declare that they have no conflict of interests.

## Acknowledgements

We are grateful for the support from the Hospital-Level Innovation and Development Fund (No. YC2021CX25).

## Funding

This study is funded by the Hospital-Level Innovation and Development Fund (No. YC2021CX25).

## Availability of Data and Materials

The datasets used and/or analyzed during the current study are available from the corresponding author on reasonable request.

## Authors' Contribution

Study concept and design: Liping Shi, Chong Zou and Tian Xie. Acquisition of data, analysis and interpretation of data: Chong Zou and Tingting Chen. Statistical analysis: Lijuan Mao. Drafting of the manuscript: Liping Shi, Tian Xie. Critical revision of the manuscript: Liping Shi, Tian Xi.

## Ethics Approval and Informed Consent

Not applicable.

## References

- Strum WB. Colorectal Adenomas. *N Engl J Med* 2016; 374: 1065-1075.
- Chen J, Bian DX, Zang SF, Yang ZX, Tian GY, Luo Y, Yang J, Xu BB, Shi JP. The association between nonalcoholic fatty liver disease and risk of colorectal adenoma and cancer incident and recurrence: a meta-analysis of observational studies. *Expert Rev Gastroenterol Hepatol* 2019; 13: 385-395.
- Schatzkin A, Lanza E, Corle D, Lance P, Iber F, Caan B, Shike M, Weissfeld J, Burt R, Cooper MR, Kikendall JW, Cahill J. Lack of effect of a low-fat, high-fiber diet on the recurrence of colorectal adenomas. Polyp Prevention Trial Study Group. *N Engl J Med* 2000; 342: 1149-1155.
- Zhao ZW, Yin ZF, Hang ZN, Zhang CJ, Zhao QC. Association between red and processed meat intake and colorectal adenoma incidence and recurrence: a systematic review and meta-analysis. *Oncotarget* 2018; 9: 32373.
- Yabuuchi Y, Imai K, Hotta K, Ito S, Kishida Y, Yoshida M, Kawata N, Kakushima N, Takizawa K, Ishiwatari H, Matsubayashi H, Aizawa D, Oishi T, Imai T, Ono H. Efficacy and safety of cold-snare endoscopic mucosal resection for colorectal adenomas 10 to 14 mm in size: a prospective observational study. *Gastrointest Endosc* 2020; 92: 1239-1246.
- Sehdev A, O'Neil BH. The Role of Aspirin, Vitamin D, Exercise, Diet, Statins, and Metformin in the Prevention and Treatment of Colorectal Cancer. *Curr Treat Options Oncol* 2015; 16: 43.
- Umezawa S, Higurashi T, Komiya Y, Arimoto J, Horita N, Kaneko T, Iwasaki M, Nakagama H, Nakajima A. Chemoprevention of colorectal cancer: Past, present, and future. *Cancer Sci* 2019; 110: 3018-3026.
- Jayakrishnan T, Abel S, Reichstein A, Fortunato R, Nosik S, McCormick J, Finley G, Monga D, Kirichenko AV, Wegner RE. Retrospective analysis of the predictors of outcome following local excision for T1 rectal adenocarcinoma. *WCRJ* 2021; 8: e2094.
- Simon K. Colorectal cancer development and advances in screening. *Clin Interv Aging* 2016; 11: 967-976.
- Okugawa Y, Grady WM, Goel A. Epigenetic Alterations in Colorectal Cancer: Emerging Biomarkers. *Gastroenterology* 2015; 149: 1204-1225.
- Mecklin JP, Aarnio M, Laara E, Kairaluoma MV, Pylvanainen K, Peltomaki P, Aaltonen LA, Jarvinen HJ. Development of colorectal tumors in colonoscopic surveillance in Lynch syndrome. *Gastroenterology* 2007; 133: 1093-1098.
- Soon WW, Hariharan M, Snyder MP. High-throughput sequencing for biology and medicine. *Mol Syst Biol* 2013; 9: 640.
- Hamfjord J, Stangeland AM, Hughes T, Skrede ML, Tveit KM, Ikdahl T, Kure EH. Differential expression of miRNAs in colorectal cancer: comparison of paired tumor tissue and adjacent normal mucosa using high-throughput sequencing. *PLoS One* 2012; 7: e34150.
- Zhu GJ, Liu F, Xu YG, Zhao CX, Zhao JG, Sun C. HMGN5 promotes invasion and migration of colorectal cancer through activating FGF/FGFR pathway. *Eur Rev Med Pharmacol Sci* 2021; 25: 1330-1338.
- Hou M, Zhang LJ, Liu J, Hu HX, Zhao YL. CircRIP2 aggravates the deterioration of colorectal carcinoma by negatively regulating CBFB. *Eur Rev Med Pharmacol Sci* 2022; 26: 3514-3521.
- Ramezani M, Aalami Aleagha Z, Almasi A, Khazaei S, Oltulu P, Sadeghi M. Expression of MSH-6 immunohistochemistry marker in colorectal cancer. *WCRJ* 2021; 8: e1989.
- Timar J, Kashofer K. Molecular epidemiology and diagnostics of KRAS mutations in human cancer. *Cancer Metastasis Rev* 2020; 39: 1029-1038.
- Gallo G, Vescio G, De Paola G, Sammarco G. Therapeutic Targets and Tumor Microenvironment in Colorectal Cancer. *J Clin Med* 2021; 10: 2295.
- Pedrosa L, Esposito F, Thomson TM, Maurel J. The Tumor Microenvironment in Colorectal Cancer Therapy. *Cancers (Basel)* 2019; 11: 1172.
- The Gene Ontology C. The Gene Ontology Resource: 20 years and still going strong. *Nucleic Acids Res* 2019; 47: 330-338.
- Kanehisa M, Furumichi M, Sato Y, Ishiguro-Watanabe M, Tanabe M. KEGG: integrating viruses

- and cellular organisms. *Nucleic Acids Res* 2021; 49: 545-551.
- 22) Szklarczyk D, Franceschini A, Wyder S, Forslund K, Heller D, Huerta-Cepas J, Simonovic M, Roth A, Santos A, Tsafou KP, Kuhn M, Bork P, Jensen LJ, von Mering C. STRING v10: protein-protein interaction networks, integrated over the tree of life. *Nucleic Acids Res* 2015; 43: 447-452.
- 23) Lin W, Wu S, Chen X, Ye Y, Weng Y, Pan Y, Chen Z, Chen L, Qiu X, Qiu S. Characterization of Hypoxia Signature to Evaluate the Tumor Immune Microenvironment and Predict Prognosis in Glioma Groups. *Front Oncol* 2020; 10: 796.
- 24) Friedman J, Hastie T, Tibshirani R. Regularization Paths for Generalized Linear Models via Coordinate Descent. *J Stat Softw* 2010; 33: 1-22.
- 25) Zhu T, Wang R, Miller H, Westerberg LS, Yang L, Guan F, Lee P, Gong Q, Chen Y, Liu C. The interaction between iNKT cells and B cells. *J Leukoc Biol* 2022; 111: 711-723.
- 26) Jiang X, Wang J, Deng X, Xiong F, Ge J, Xiang B, Wu X, Ma J, Zhou M, Li X. Role of the tumor microenvironment in PD-L1/PD-1-mediated tumor immune escape. *Mol Cancer* 2019; 18: 1-17.
- 27) Yao H, Lan J, Li C, Shi H, Brosseau JP, Wang H, Lu H, Fang C, Zhang Y, Liang L. Inhibiting PD-L1 palmitoylation enhances T-cell immune responses against tumours. *Nat Biomed Eng* 2019; 3: 306-317.
- 28) Garg M, Shanmugam MK, Bhardwaj V, Goel A, Gupta R, Sharma A, Baligar PK, Alan PG, Boon C, Wang, L. The pleiotropic role of transcription factor STAT3 in oncogenesis and its targeting through natural products for cancer prevention and therapy. *Med Res Rev* 2021; 41: 1291-1336.
- 29) Harvie M. Nutritional supplements and cancer: potential benefits and proven harms. *Am Soc Clin Oncol Educ Book* 2014: e478-486.
- 30) Doll D, Keller L, Maak M, Boulesteix AL, Siewert JR, Holzmann B, Janssen KP. Differential expression of the chemokines GRO-2, GRO-3, and interleukin-8 in colon cancer and their impact on metastatic disease and survival. *Int J Colorectal Dis* 2010; 25: 573-581.
- 31) Liu WQ, Li WL, Ma SM, Liang L, Kou ZY, Yang J. Discovery of core gene families associated with liver metastasis in colorectal cancer and regulatory roles in tumor cell immune infiltration. *Transl Oncol* 2021; 14: 101011.
- 32) Yin TF, Zhao DY, Zhou YC, Wang QQ, Yao SK. Identification of the circRNA-miRNA-mRNA regulatory network and its prognostic effect in colorectal cancer. *World J Clin Cases* 2021; 9: 4520-4541.
- 33) Wu Q, Yan T, Chen Y, Chang J, Jiang Y, Zhu D, Wei Y. Integrated Analysis of Expression and Prognostic Values of Acyl-CoA Dehydrogenase short-chain in Colorectal Cancer. *Int J Med Sci* 2021; 18: 3631-3643.
- 34) Tian Y, Song W, Li D, Cai L, Zhao Y. Resveratrol as a natural regulator of autophagy for prevention and treatment of cancer. *OncoTargets and therapy* 2019; 12: 8601-8609.
- 35) Boursi B, Haynes K, Mamtani R, Yang YX. Thyroid dysfunction, thyroid hormone replacement and colorectal cancer risk. *J Natl Cancer Inst* 2015; 107: djv084.
- 36) Du G, Fang X, Dai W, Zhang R, Liu R, Dang X. Comparative gene expression profiling of normal and human colorectal adenomatous tissues. *Oncol Lett* 2014; 8: 2081-2085.
- 37) Helm JF, Russo MW, Biddle AK, Simpson KN, Ransohoff DF, Sandler RS. Effectiveness and economic impact of screening for colorectal cancer by mass fecal occult blood testing. *Am J Gastroenterol* 2000; 95: 3250-3258.
- 38) Lu D, Dong D, Zhou Y, Lu M, Pang XW, Li Y, Tian XJ, Zhang Y, Zhang J. The tumor-suppressive function of UNC5D and its repressed expression in renal cell carcinoma. *Clin Cancer Res* 2013; 19: 2883-2892.
- 39) Dong D, Zhang L, Bai C, Ma N, Ji W, Jia L, Zhang A, Zhang P, Ren L, Zhou Y. UNC5D, suppressed by promoter hypermethylation, inhibits cell metastasis by activating death-associated protein kinase 1 in prostate cancer. *Cancer Sci* 2019; 110: 1244-1255.
- 40) Zhang MM, Sun F, Cui B, Zhang LL, Fang Y, Li Y, Zhang RJ, Ye XP, Ma YR, Han B, Song HD. Tumor-suppressive function of UNC5D in papillary thyroid cancer. *Oncotarget* 2017; 8: 96126-96138.
- 41) Lu YC, Nazarko OV, Sando III R, Salzman GS, Li NS, Südhof TC, Araç D. Structural basis of latrophilin-FLRT-UNC5 interaction in cell adhesion. *Structure* 2015; 23: 1678-1691.
- 42) Uhan S, Zidar N, Tomazic A, Hauptman N. Hypermethylated promoters of genes UNC5D and KCNA1 as potential novel diagnostic biomarkers in colorectal cancer. *Epigenomics* 2020; 12: 1677-1688.